Water Air Soil Pollut (2024) 235:116
https://doi.org/10.1007/s11270-024-06921-z

Study on Self-cementation Solidification of Heavy Metals in Municipal Solid Waste Incineration Fly Ash by Alkali-activation

Lin Yu · Dongwei Li

Received: 30 October 2022 / Accepted: 17 January 2024 / Published online: 29 January 2024

Abstract Municipal solid waste incineration (MSWI) fly ash is considered hazardous waste due to heavy metals. Their improper management/disposal is lethal for both humans and animals. This paper aims to explore the gelling properties of fly ash, activated by adding different alkali activators, i.e., Na_2SiO_3, NaOH, KOH, Na_2SiO_3:NaOH (1:1, g/g), and Na_2SiO_3:KOH(1:1, g/g). The optimum result was achieved using a composite alkali-activator of Na_2SiO_3-NaOH, based on a single-factor experiment. Therefore, the influence of alkali-activators/fly ashes (A/M), Na_2SiO_3/NaOH, and liquid/solid (L/S) ratios on the fixation of heavy metals and compressive strength has been investigated by an orthogonal procedure. The optimal combination of these factors is achieved at the following ratios; 14.2% of A/M, 7/3 (g/g) of Na_2SiO_3/NaOH, and 0.43 (mL/g) of L/S. Solidification mechanism and heavy metals fixation in the solidified body containing C-S–H and C-A-S–H gels are determined by X-ray diffraction (XRD), scanning electron microscope (SEM), and Fourier transform infrared spectroscopy (FTIR).

L. Yu · D. Li (✉)
State Key Laboratory for Coal Mine Disaster Dynamics and Control, Chongqing University, Chongqing 400044, People's Republic of China
e-mail: litonwei@cqu.edu.cn

L. Yu
Chongqing Metropolitan College of Science and Technology, Chongqing 402160, People's Republic of China

Keywords Immobilization · Compressive Strength · Solidified Samples · Leaching · Mechanism

1 Introduction

The toxicity of Municipal Solid Waste Incineration (MSWI) fly ash is because of heavy metals (HMs) and persistent organic contaminants present in it, which deteriorate the ecological environment and human health (Lin et al., 2021; Wang et al., 2022a; Zhang et al., 2022). The MSWI fly ash contains teratogenic and carcinogenic contaminants such as lead, zinc, copper, cadmium, and dissolved salts. The environmental factor is the discharge of heavy metals from mishandled MSWI fly ash in the environment (Li et al., 2016; Pan et al., 2022). Several methods are used to treat MSWI fly ash, including landfill, chemical separation, sintering, fusion, solidification/stabilization (S/S) (Guo & Shi, 2013; Zheng et al., 2022). The landfill is not economical due to the utilization of more land (Huang et al., 2015). The chemical separation process extracts higher concentrations of heavy metals using chemical extraction and biological leaching techniques and allows them to be recycled after treatment. The solidification/stabilization process mainly uses cement, asphalt, melting (high-temperature treatment), chemicals, etc., to immobilize heavy metals (Bashar et al., 2014; Hwang & Huynh, 2015; Leong et al., 2016; Xu et al., 2022). Solidification of MSWI fly ash immobilizes heavy metals and other pollutants by adding chemically active substances (Quina et al., 2018;

Wang et al., 2015a; Xue et al., 2012). According to US Environmental Protection Agency solidification/stabilization is best technology for treatment of toxic and hazardous waste (Asavapisit et al., 2005; Malviya & Chaudhary, 2006; Yoon et al., 2010). So this method is of great interest for researchers and scholars all over the world (Bai et al., 2022; Chen et al., 2022; Wang et al., 2022b).

A lot of work has been conducted on the solidification of heavy metals in fly ash using cement or slag and achieved good results, but the gel-like characteristics of fly ash were ignored for a long. Using slag or cement to solidify fly ash is not only a compaction problem but also a large volume of land for its disposal (Poon et al., 2006; Zheng et al., 2011). Due to gelatin activity, fly ash on hydration reaction generates ettringite, which enhances the compressive strength of the body (Zhao et al., 2002). Moreover, Fly ash with pozzolanic activity contains a certain amount of active silica, alumina, and other components. Adding an alkali activator in fly ash generates hydrated calcium silicate and aluminate or hydrated calcium aluminate reaction products (Wei et al., 2011). These properties and reactions provide a theoretical basis for the solidification of fly ash. The solidification of the fly ash by the alkali activator has no problem with compaction (Wang et al., 2016). Using fly ash as a solidification/stabilization of heavy metals is an economical and simple process and has a great advantage over other techniques (Wang et al., 2015b).

In this paper, a composite alkali-activator is selected to immobilize the HMs in MSWI fly ash. The gel properties of MSWI fly ash are similar to those found in coal ash. So fly ash is solidified and stabilized with the moderate addition of sodium silicate (i.e., Na_2SiO_3) and sodium hydroxide (i.e., NaOH) in the current experiment. A single-factor experiment is conducted to determine the appropriate combination of alkali-activators. Orthogonal tests are designed to analyze the optimal set of the experimental parameters; (a) mass ratio of alkali-activators and fly ashes (A/M ratio), (b) Na_2SiO_3 to NaOH ratio (i.e., Na_2SiO_3/NaOH) and (c) proportion of water to the solid mixture (i.e., L/S ratio). The X-ray diffraction (XRD), scanning electron microscope (SEM), and Fourier transform infrared spectroscopy (FTIR) are used to understand the solidification mechanism.

2 Materials and Experimental Methods

2.1 Materials Preparation

Municipal solid waste incineration fly ash used in this study was obtained from a waste incineration power generation plant in Chongqing, China. Fly ash samples were sieved through 200-mesh after being dried at 60 ℃ for 6 h. All experiments were performed using triplets of samples from the same batches of materials. Distilled water was used throughout the experiment. The raw materials of chemical composition were analyzed using X-ray fluorescence (XRF Shimadzu, PerkinElmer), and the results are listed in Table 1. The particle size distribution of the fly ash specimen is shown in Fig. 1.

2.2 Preparation of Solidified Body

The certain proportion of the MSWI fly ash, alkali-activators, and distilled water was mixed, and was evenly stirred until cooled to room temperature. The slurry was then shifted into a 20 mm×20 mm×20 mm steel

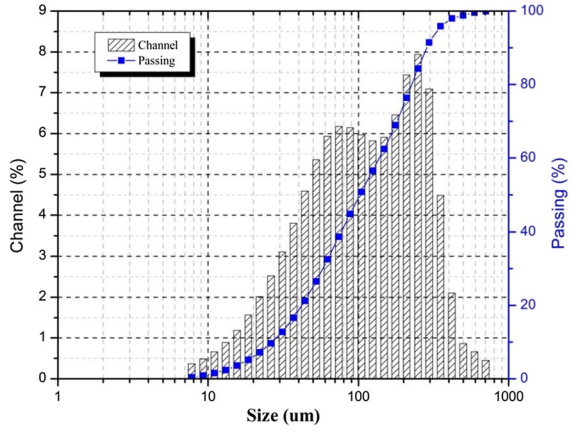

Fig. 1 Particle size distribution of raw fly ashes

Table 1 Chemical compositions of the raw MSWI fly ash (w/%)

CaO	Cl	SiO_2	Na_2O	SO_3	K_2O	MgO	Al_2O_3	Fe_2O_3	P_2O_5	ZnO	PbO	CuO
52.50	17.44	6.01	5.83	4.98	4.19	2,49	1.92	1.4	0.92	0.85	0.27	0.10

mold and vibrated for 10 min. The preparation process of solidified body is shown in Fig. 2. The solid specimens were removed from the mold after 24 h and then restored to the indoor environment for 28 days.

2.3 Leaching and Compressive Strength Tests

The leaching toxicity test of solidified samples were prepared according to Chinese standard HJ/T300-2007 entitled "The leaching toxicity of solid waste-Acetic acid buffer solution method." The pulverized sample particles were sieved (Φ 9.5 mm) and added to the prepared chemical regents (glacial acetic acid solution) at a mass-liquid ratio of 20:1 (g/mL). The mixture was shaken and tumbled at a speed of 30 ± 2 rpm for 18 ± 2 h at 23 ± 2℃ in an oscillating device. Then leachate of the samples was filtrated through a micro-porous filter membrane (Φ 0.8 μm), and leaching concentrations of HMs (Zn, Pb, Cu, and Cd) were detected using an atomic absorption spectrophotometer (TAS-999). The compressive strengths of solidified specimens were measured according to Chinese standard GB/T 17671–1999 using a universal testing machine (AGN-250) with a 10% standard deviation. All experiments were conducted with triplicate specimens after 28 days.

2.4 Analytical Methods

The raw samples and solidified bodies were scanned by the X-ray diffraction (PANalytical B.V., Holland) at CuK α radiation generated at 30 mA and 40 kV with 2θ ranging from 10° to 90°. Morphology of samples was obtained using Scanning Electron Microscopy (SEM, Carl Zeiss AG, Germany) at an accelerating voltage of 20 kV. Fourier transform infrared spectroscopy analysis was performed using Fourier Transform Infrared spectroscopy (Nicolet5DXC FT-IR) in the range of 400–4000 cm^{-1}.

3 Results and Discussions

3.1 Alkali-activator Comparison

The alkali-activators used in solidifying wastes include Na_2SiO_3, K_2SiO_3, NaOH, and KOH. Single-factor experiments were designed to select suitable alkali activators for immobilizing heavy metals in fly ash using Na_2SiO_3, NaOH, KOH, Na_2SiO_3:NaOH(1:1, g/g), and Na_2SiO_3:KOH(1:1, g/g). A total of 100 g alkali-activator and 40 mL distilled water were used in each set of experiments with three replicates specimens. The influence of different alkali-activators on the leaching concentration of HMs presented in Fig. 3. It concluded from Fig. 3 that in the case of Na_2SiO_3-NaOH; the leaching concentration of Cu, Zn, and Cd was lower than the other four alkali-activators. While minimum leaching concentration of Pb ions was observed by using NaOH as an alkali-activator in contrast to other activators. Since there is no significant difference in the leaching concentration of Pb resulting from NaOH and

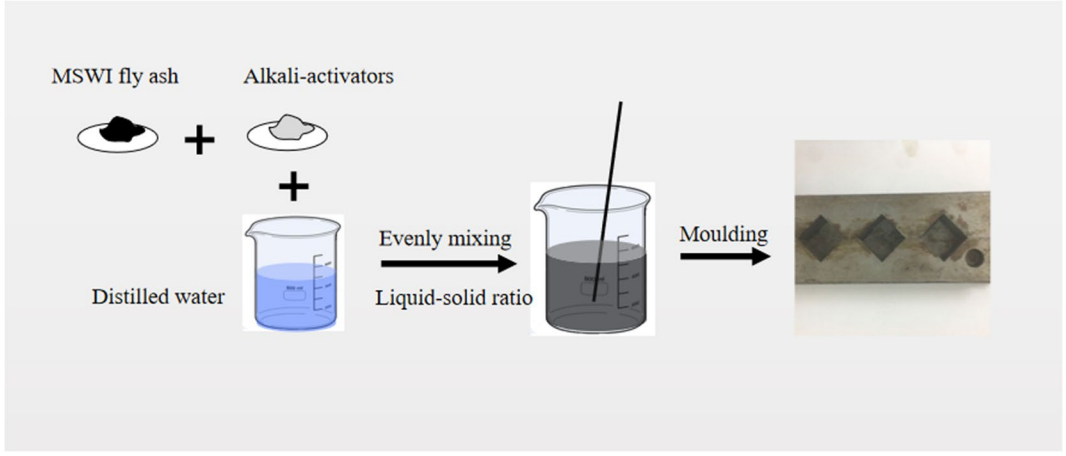

Fig. 2 The preparation process of solidified body

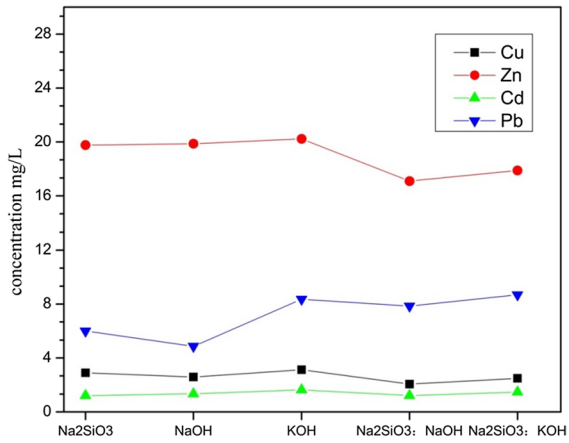

Fig. 3 The effects of different alkali-activators on the leaching concentration of HMs

Na_2SiO_3, the lowest leaching concentration may be obtained by adjusting the mass ratio of Na_2SiO_3 and NaOH in Na_2SiO_3-NaOH.

3.2 Optimization Analysis

The fixation rate of the HMs and the compressive strength of the solidified bodies measured in orthogonal experiments were used to quantify the influence of A/M, Na_2SiO_3/NaOH, and L/S ratios on the S/S performance of fly ashes. The fixation rate of the HM directly reflects the decrease in the leaching concentration from the solidified body as compared to the original sample, which is expressed in the following equation:

$$y = (U1 - U2)/U1 \times 100\% \quad (1)$$

where y is the fixation rate of the heavy metal and U1 and U2 denote the leaching concentrations from the raw sample and solidified body, respectively. The design of orthogonal experiments and the fixation results are shown in Tables 2 and 3, respectively. The leaching concentration of HMs in the raw fly ashes and the solidified body samples in the orthogonal tests are presented in Table 4.

It was seen from Table 3 that the maximum fixation rate of elements Cu, Zn, Cd, and Pb in 9 groups of tests was 86.96%, 22.35%, 61.31%, and 64.91%, respectively, and the corresponding leaching concentrations were 2.60 mg/L, 18.58 mg/L, 1.48 mg/L, and 7.22 mg/L, respectively. The optimum solidification of Cu was observed at A3B3C3; A3 (9.1% A/M ratio), B3 (7/3 Na_2SiO_3/NaOH ratio) and C3 (0.47 L/S ratio). The highest fixation rates of Zn and Cd were examined at A2B3C1; the highest fixation rate of Pb was examined at A1B1C1. Based on the ranking of three factors, A, B, and C, for the four HM elements and the R-value analysis, the best parameters combination achieved at A1B3C1; A/M ratio of 14.2% (A1), Na_2SiO_3/NaOH ratio of 7/3 (B3) and L/S ratio of 0.43 (C1). In the current study, the highest compressive strength of solidified body was 1.025 MPa. The optimum combination regarding compressive strength (0.68 MPa) was observed at A3B3C3. The difference in the compressive strength of the solidified body was not significant at L/S ratios of 0.47 vs. 0.43 and A/M ratios of 14.2% vs. 9.1%.

3.3 Mineral phase analysis

Hydration products were determined by XRD (Fig. 4) and were one of the main factors in determining the

Table 2 Orthogonal experiment matrix

No. T-j	A	B	C	Fixation rate (%)				Compressive strength / MPa
				Cu	Zn	Cd	Pb	
T1	1 (14.2%)	1 (6/4)	1 (0.43)	84.38	17.44	56.00	60.99	0.600
T2	1	2(1/1)	2 (0.45)	85.58	18.89	58.99	61.26	0.425
T3	1	3(7/3)	3 (0.47)	85.17	16.21	52.92	64.91	0.800
T4	2 (11.1%)	1	2	83.75	15.00	53.09	60.98	0.450
T5	2	2	3	84.36	18.75	54.21	54.27	0.500
T6	2	3	1	86.57	22.35	61.31	61.98	0.850
T7	3 (9.1%)	1	3	86.96	16.54	49.72	58.43	0.775
T8	3	2	1	85.51	13.77	49.77	60.62	1.025
T9	3	3	2	84.55	18.56	52.79	50.81	0.675

A mass ratio of alkali-activators and fly ashes (g/g), *B* Na_2SiO_3-NaOH mass ratio (g/g), *C* liquid–solid ratio (mL/g)

Table 3 The range analysis of fixation rate and compressive strength

	Cu			Zn			Cd			Pb			Compressive strength / MPa		
	A	B	C	A	B	C	A	B	C	A	B	C	A	B	C
Kj1	255.13	255.09	256.46	52.54	48.98	53.56	167.91	158.81	170.1	187.16	180.40	183.59	1.825	1.825	2.475
KJ2	254.68	255.45	253.88	56.1	51.41	52.45	168.61	162.97	164.87	177.23	176.15	173.05	1.800	1.950	1.550
Kj3	257.02	256.29	256.49	48.87	57.12	51.5	152.28	167.02	156.85	169.86	177.7	177.61	2.475	2.325	2.075
kj1	85.04	85.03	85.49	17.51	16.33	17.85	55.97	52.94	55.69	63.72	60.13	61.20	0.608	0.608	0.823
kj2	84.89	85.15	84.63	18.7	17.14	17.48	56.20	54.32	54.96	59.08	58.72	57.68	0.600	0.650	0.517
kj3	85.67	85.43	85.5	16.28	19.04	17.17	50.76	55.67	52.28	56.62	59.23	59.20	0.825	0.775	0.692
Optimal level	A3	B3	C3	A2	B3	C1	A2	B3	C1	A1	B1	C1	A3	B3	C3
R	0.78	0.40	0.87	2.24	2.71	0.68	5.44	2.73	3.41	7.10	1.42	3.52	0.225	0.167	0.306
Order	C > A > B			B > A > C			A > C > B			A > C > B			C > A > B		

A A/M ratio (g/g), *B* Na_2SiO_3/NaOH mass ratio (g/g); C: L/S ratio (mL/g), K_{ji} *(i = 1, 2, 3)* summation of the testing values in the same level; k_{ji} (i = 1, 2, 3) = 1/3*Kji

Table 4 The leaching concentration (mg/L) of HMs

No	Cu	Zn	Cd	Pb
0[a]	17.605	22.518	3.241	18.107
1[b]	2.751	18.59	1.426	6.340
2[c]	2.538	18.265	1.329	7.016
3[d]	2.611	18.868	1.526	6.355
4[e]	2.824	19.139	1.521	7.065
5[f]	2.754	18.297	1.484	8.280
6[g]	2.364	17.485	1.254	6.885
7[h]	2.297	18.794	1.629	6.983
8[i]	2.551	19.417	1.628	7.130
9[j]	2.720	18.339	1.530	8.906

[a]Raw MSWI fly ashes

[b–j]The solidified body samples

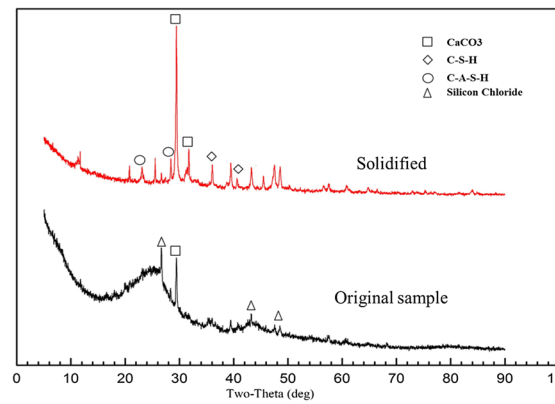

Fig. 4 The XRD patterns of the original sample and the solidified body

leaching properties of heavy metals in the solidified body. The main phases in the original samples were calcium carbonate ($CaCO_3$) and silicon chloride ($SiCl_4$). While in the case of the solidified body, the main mineral phases were calcium silicoaluminate hydrate ($2CaO{\cdot}Al_2O_3{\cdot}SiO_2{\cdot}8H_2O$), denoted as C-A-S–H, and the calcium silicate hydrate ($CaO{\cdot}SiO_2{\cdot}nH_2O$) represented as C-S–H.

Some aluminum atoms in C-A-S–H bonded with silicon and formed a two-dimensional network structure, which had a large specific surface area and pore volume. The greater specific surface area led to an increase in the cation exchange capacity of C-A-S–H. It ultimately enhanced heavy metals' solidification/stabilization ability in the fly ash grains. At the same

time, C-S–H has a stratified structure with lower degrees of polymerizations for the silicon and has a great specific surface area and pore volume. In addition, it has a high unsaturated surface potential which strongly bound water molecules, and the high density of irregular hydrogen bonding caused the stronger adsorption of HMs on the polymer surface.

3.4 Morphology analysis

As shown in Fig. 5a, the original MSWI fly ashes consist of fine particles with a hollow and sparse appearance. The flocculation of particles resulted in amorphous and polycrystalline aggregates. Moreover, it also contained tabular and layered structures. The surface of the particles was not smooth, with many raised and hollow structures indicating clear network structures. While in the case of the solidified body, dense grid structures were observed as a result of Si–O, Ca-O, and H–O reactions (Fig. 5b). Therefore, the solidified body has a smaller surface area and lower permeability, indicating that contaminants were more strongly adsorbed and difficult to be leached.

3.5 FTIR analysis

The infrared spectrum of the solidified body shown in Fig. 6 indicates that each hydration product exhibited a similar absorption band. The absorption peaks were observed at 3441 cm^{-1} (bending vibration), 1622 cm^{-1} (bending vibration), and 1444 cm^{-1} (stretching vibration), which ensured the presence of O–H (γ OH), middle water H–O-H (γ $2H_2O$), and O-C-O ions respectively in the solidified body. The absorption peaks at 873 cm^{-1} were due to Al–OH symmetric structure. Si–O (γ3) presence is observed at 1000 cm^{-1} (asymmetric stretching vibration) absorption peaks. While the absorption bands at 458 cm^{-1}, 1121 cm^{-1}, and 1156 cm^{-1} correspond to Si–O inner surface bending vibration. The above analysis confirmed that the solidified body's hydration reaction occurred under the calcium aluminosilicate hydrate wave (C-A-S–H).

3.6 Mechanism exploration

XRD, SEM, and FTIR analyses indicate that the alkali-activator significantly influenced the immobilization of the HMs in MSWI fly ash. The pozzolanic behavior of coal ash is mainly due to CaO-SiO_2. During the alkali activation, the fly ash particles rapidly dissolved, resulting in active components; SiO_2 and Al_2O_3 released. This mechanism leads to the encapsulation of heavy metals by C-S–H and C-A-S–H present in a hard solid matrix. Furthermore, heavy metals combined either with OH^- or silicate to form calcium salts, which adsorbed on C-S–H and became components of crystal structure. In the current study, Zn^{2+} and Cu^{2+} replaced the Ca^{2+} of C-S–H or reacted on the surface of particles, forming the oxides of Ca^{2+} and Zn^{2+} or Cu^{2+}. In the meantime, Cd^{2+} would be precipitated into $Ca(OH)_2$. The immobilization process of Pb^{2+} can be described as follows:

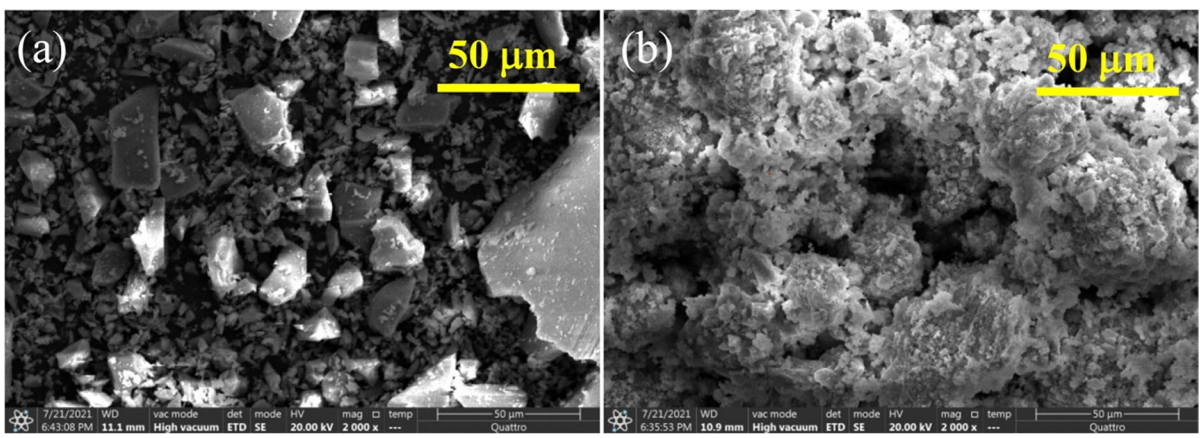

Fig. 5 The morphology of the raw MSWI fly ash and the solidified body (**a** a raw MSWI fly ash; **b** solidified body)

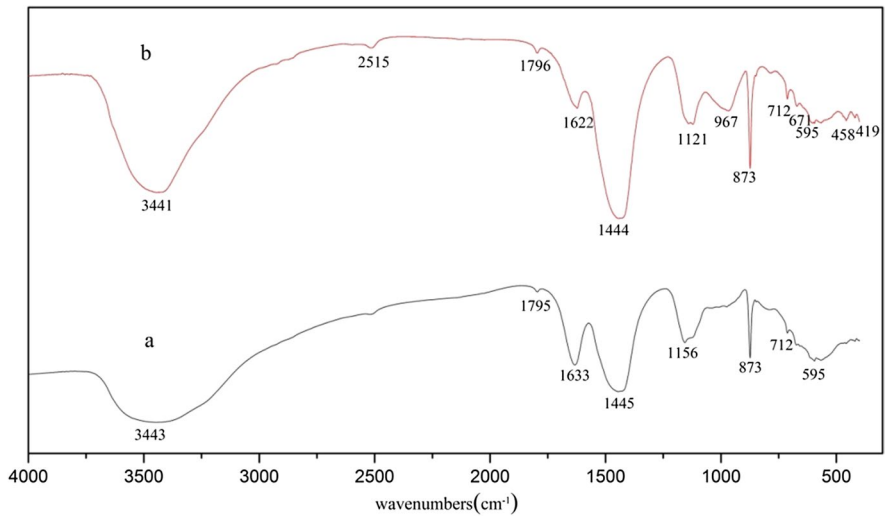

Fig. 6 The FTIR spectra of the original sample (**a**) and the solidified body (**b**)

Adsorption : $C-S-H+Pb^{2+} \rightarrow Pb-C-S-H$

Isomorphous substitution : $C-S-H+Pb^{2+} \rightarrow Pb-C-S-H+Ca^{2+}$

Precipitation reaction : $Pb^{2+}+2OH^{-}+Ca^{2+}+SO_4^{2+} \rightarrow$ double salt

4 Conclusions

The medium diameter of the particle size for the MSWI fly ash is approximately 73.6 μm, with a range varying between 50 and 500 μm. The heavy metals detected in the raw samples are trace elements of Pb, Zn, Cd, and Cu. The main components responsible for pozzolanic activity are CaO-SiO_2 in MSWI fly ash. The Municipal solid waste incineration fly ash potentially has tephra properties, which possess some specific gelling properties. Their gelling properties are activated by adding alkali-activators, and thus fly ashes solidified. In this paper, alkali-activator Na_2SiO_3 + NaOH (1:1, g/g) was selected for further investigation of the immobilization of HMs due to their lower leaching concentration. Based on results, fixation rate, and compressive strengths, the optimum selected parameters were; A1 (A/M ratio of 14.2%), B3 (Na_2SiO_3/NaOH ratio of 7/3), and C1(L/S ratio of 0.43) forming a combination of A1B3C1. The difference in compressive strength of solidified bodies was not significant between A1 (14.2%) and A3 (9.1%); the difference in compressive strength of solidified bodies was not significant between C1 (0.43) and C3 (0.47). The main hydration products of the solidified body of the fly ashes were C-S–H and C-A-S–H. The immobilization mechanism of the four HM elements was as follows; Zn^{2+} and Cu^{2+} replaced Ca^{2+} or reacted with Ca^{2+} on the surface of C-S–H to form the oxides of calcium, zinc, or copper in the hydration process. While Cd is incorporated into the gel of the calcium *hydroxide (i.e., Ca*$(OH)_2$) through co-precipitation and Pb solidified in the C-S–H gel through a combined process of the adsorption, isomorphic substitution, and precipitation reaction. This study demonstrated that the solidification of heavy metals in municipal solid waste incinerators flies ash is achieved by alkali activations.

Author contribution Lin Yu conceived and designed the experiments; Lin Yu performed the experiments; Lin Yu analyzed the data; Lin Yu contributed reagents/materials/analysis tools; Lin Yu wrote the paper. Dongwei Li supervised the project.

Funding I have received the grant supporting research work and funds to cover publishing costs in open access. This work was supported by the National Natural Science Foundation of China under Grant NO.51274262.

Data availability The data that support the findings of this study are available from the corresponding author, Dongwei Li, upon reasonable request.

Declarations

Conflict of interest The authors declare no competing interests.

References

Asavapisit, S., Naksrichum, S., & Harnwajanawong, N. (2005). Strength, leachability and microstructure characteristics of cement-based solidified plating sludge. *Cement and Concrete Research, 35*(6), 1042–1049. https://doi.org/10.1016/j.cemconres.2004.07.041

Bai, Y., Guo, W., Wang, X., Pan, H., Zhao, Q., & Wang, D. (2022). Utilization of municipal solid waste incineration fly ash with red mud-carbide slag for eco-friendly geopolymer preparation. *Journal of Cleaner Production, 340*, 130820. https://doi.org/10.1016/j.jclepro.2022.130820

Bashar, I. I., Alengaram, U. J., Jumaat, M. Z., & Islam, A. (2014). The Effect of variation of molarity of alkali activator and fine aggregate content on the compressive strength of the fly ash: Palm oil fuel ash based geopolymer mortar. *Advances in Materials Science and Engineering, 2014*, e245473. https://doi.org/10.1155/2014/245473

Chen, L., Wang, L., Zhang, Y., Ruan, S., Mechtcherine, V., & Tsang, D. C. W. (2022). Roles of biochar in cement-based stabilization/solidification of municipal solid waste incineration fly ash. *Chemical Engineering Journal, 430*, 132972. https://doi.org/10.1016/j.cej.2021.132972

Guo, X., & Shi, H. (2013). Self-solidification/stabilization of heavy metal wastes of class C fly ash–based geopolymers. *Journal of Materials in Civil Engineering, 25*(4), 491–496. https://doi.org/10.1061/(ASCE)MT.1943-5533.0000595

Huang, T., Li, D., Kexiang, L., & Zhang, Y. (2015). Heavy metal removal from MSWI fly ash by electrokinetic remediation coupled with a permeable activated charcoal reactive barrier. *Scientific Reports, 5*(1), 15412. https://doi.org/10.1038/srep15412

Hwang, C.-L., & Huynh, T.-P. (2015). Effect of alkali-activator and rice husk ash content on strength development of fly ash and residual rice husk ash-based geopolymers. *Construction and Building Materials, 101*, 1–9. https://doi.org/10.1016/j.conbuildmat.2015.10.025

Leong, H. Y., Ong, D. E. L., Sanjayan, J. G., & Nazari, A. (2016). The effect of different Na2O and K2O ratios of alkali activator on compressive strength of fly ash based-geopolymer. *Construction and Building Materials, 106*, 500–511. https://doi.org/10.1016/j.conbuildmat.2015.12.141

Li, D., Huang, T., & Liu, K. (2016). Near-anode focusing phenomenon caused by the coupling effect of early precipitation and backward electromigration in electrokinetic remediation of MSWI fly ashes. *Environmental Technology, 37*(2), 216–227. https://doi.org/10.1080/09593330.2015.1066873

Lin, H., Zhang, P., Zeng, L., Jiao, B., Shiau, Y., & Li, D. (2021). Preparation of glass-ceramics via cosintering and solidification of hazardous waste incineration residue and chromium-containing sludge. *ACS Omega, 6*(37), 23723–23730. https://doi.org/10.1021/acsomega.1c01659

Malviya, R., & Chaudhary, R. (2006). Factors affecting hazardous waste solidification/stabilization: A review. *Journal of Hazardous Materials, 137*(1), 267–276. https://doi.org/10.1016/j.jhazmat.2006.01.065

Pan, S., Ding, J., Peng, Y., Lu, S., & Li, X. (2022). Investigation of mechanochemically treated municipal solid waste incineration fly ash as replacement for cement. *Energies, 15*(6), 2013. https://doi.org/10.3390/en15062013

Poon, C. S., Qiao, X. C., Cheeseman, C. R., & Lin, Z. S. (2006). Feasibility of using reject fly ash in cement-based stabilization/solidification processes. *Environmental Engineering Science, 23*(1), 14–23. https://doi.org/10.1089/ees.2006.23.14

Quina, M., Bontempi, E., Bogush, A., Schlumberger, S., Weibel, G., Braga, R., et al. (2018). Technologies for the management of MSW incineration ashes from gas cleaning: New perspectives on recovery of secondary raw materials and circular economy. *The Science of the Total Environment, 635*, 526–542. https://doi.org/10.1016/j.scitotenv.2018.04.150

Wang, C. P., Li, F. Z., Zhou, M. K., Chen, Y., & Chen, X. (2015). Effect of cement-MSWI fly ash hydration on the stabilisation/solidification of Pb and Cd. *Materials Research Innovations, 19*(5), S5-1161-S5-1166. https://doi.org/10.1179/1432891714Z.0000000001270

Wang, F.-H., Zhang, F., Chen, Y.-J., Gao, J., & Zhao, B. (2015b). A comparative study on the heavy metal solidification/stabilization performance of four chemical solidifying agents in municipal solid waste incineration fly ash. *Journal of Hazardous Materials, 300*, 451–458. https://doi.org/10.1016/j.jhazmat.2015.07.037

Wang, L., Jamro, I. A., Chen, Q., Li, S., Luan, J., & Yang, T. (2016). Immobilization of trace elements in municipal solid waste incinerator (MSWI) fly ash by producing calcium sulphoaluminate cement after carbonation and washing. *Waste Management & Research, 34*(3), 184–194. https://doi.org/10.1177/0734242X15617846

Wang, L., Zhang, Y., Chen, L., Guo, B., Tan, Y., Sasaki, K., & Tsang, D. C. W. (2022a). Designing novel magnesium oxysulfate cement for stabilization/solidification of municipal solid waste incineration fly ash. *Journal of Hazardous Materials, 423*, 127025. https://doi.org/10.1016/j.jhazmat.2021.127025

Wang, X., Zhu, K., Zhang, L., Li, A., Chen, C., Huang, J., & Zhang, Y. (2022b). Mechanical property and heavy metal leaching behavior enhancement of municipal solid waste incineration fly ash during the pressure-assisted sintering treatment. *Journal of Environmental Management, 301*, 113856. https://doi.org/10.1016/j.jenvman.2021.113856

Wei, G. X., Liu, H. Q., & Zhang, S. G. (2011). Using of different type cement in solidification/stabilization of MSWI fly ash. *Advanced Materials Research, 291–294*, 1870–1874. https://doi.org/10.4028/www.scientific.net/AMR.291-294.1870

Xu, D., Huang, Y., Jin, X., & Sun, T. (2022). Synergistic treatment of heavy metals in municipal solid waste incineration fly ash with geopolymer and chemical stabilizers. *Process Safety and Environmental Protection, 160*, 763–774. https://doi.org/10.1016/j.psep.2022.02.052

Xue, Q., Li, J., & Hu, Z. (2012). Compound stabilization/solidification of MSWI fly ash with trimercapto-s-triazine and cement. *Water Science and Technology, 66*(3), 689–694. https://doi.org/10.2166/wst.2012.226

Yoon, I.-H., Moon, D. H., Kim, K.-W., Lee, K.-Y., Lee, J.-H., & Kim, M. G. (2010). Mechanism for the stabilization/solidification of arsenic-contaminated soils with Portland cement and cement kiln dust. *Journal of Environmental Management, 91*(11), 2322–2328. https://doi.org/10.1016/j.jenvman.2010.06.018

Zhang, Z., Wang, Y., Zhang, Y., Shen, B., Ma, J., & Liu, L. (2022). Stabilization of heavy metals in municipal solid waste incineration fly ash via hydrothermal treatment with coal fly ash. *Waste Management, 144*, 285–293. https://doi.org/10.1016/j.wasman.2022.03.022

Zhao, Y., Lijie, S., & Guojian, L. (2002). Chemical stabilization of MSW incinerator fly ashes. *Journal of Hazardous Materials, 95*(1), 47–63. https://doi.org/10.1016/S0304-3894(02)00002-X

Zheng, L., Wang, C., Wang, W., Shi, Y., & Gao, X. (2011). Immobilization of MSWI fly ash through geopolymerization: Effects of water-wash. *Waste Management, 31*(2), 311–317. https://doi.org/10.1016/j.wasman.2010.05.015

Zheng, R., Wang, Y., Liu, Z., Zhou, J., Yue, Y., & Qian, G. (2022). Environmental and economic performances of municipal solid waste incineration fly ash low-temperature utilization: An integrated hybrid life cycle assessment. *Journal of Cleaner Production, 340*, 130680. https://doi.org/10.1016/j.jclepro.2022.130680